Standing-Gradient Osmotic Flow

A mechanism for coupling of water and solute transport in epithelia

JARED M. DIAMOND and WILLIAM H. BOSSERT

From the Department of Physiology, University of California at Los Angeles School of Medicine, Los Angeles, California 90024, and the Biological Laboratories, Harvard University, Cambridge, Massachusetts 02138

ABSTRACT At the ultrastructural level, epithelia performing solute-linked water transport possess long, narrow channels open at one end and closed at the other, which may constitute the fluid transport route (e.g., lateral intercellular spaces, basal infoldings, intracellular canaliculi, and brush-border microvilli). Active solute transport into such folded structures would establish standing osmotic gradients, causing a progressive approach to osmotic equilibrium along the channel's length. The behavior of a simple standing-gradient flow system has therefore been analyzed mathematically because of its potential physiological significance. The osmolarity of the fluid emerging from the channel's open end depends upon five parameters: channel length, radius, and water permeability, and solute transport rate and diffusion coefficient. For ranges of values of these parameters encountered experimentally in epithelia, the emergent osmolarity is found by calculation to range from isotonic to a few times isotonic; i.e., the range encountered in epithelial absorbates and secretions. The transported fluid becomes more isotonic as channel radius or solute diffusion coefficient is decreased, or as channel length or water permeability is increased. Given appropriate parameters, a standing-gradient system can yield hypertonic fluids whose osmolarities are virtually independent of transport rate over a wide range, as in distal tubule and avian salt gland. The results suggest that water-to-solute coupling in epithelia is due to the ultrastructural geometry of the transport route.

The purpose of this paper is to examine whether some distinctive physiological properties of epithelia might arise as geometrical consequences of epithelial ultrastructure.

Most epithelia absorb or secrete specific fluids, such as bile, the glomerular filtrate, gastric juice, aqueous humour, sweat, and cerebrospinal fluid. The primary transported fluid may be either isotonic or hypertonic to plasma (hypotonic secretions in vertebrates appear to result from isotonic secretion

followed by hypertonic reabsorption). Physiological experiments have indicated that water transport is a passive and secondary consequence of local osmotic gradients set up within the epithelium by active transport of some solute (e.g., NaCl in the gall bladder, HCl in the stomach, and bile salt in the liver). Nevertheless, there are unresolved quantitative problems raised by this water-to-solute coupling. For example, one might expect actively transported solute to tend to diffuse away from the transporting cells before its osmotic equilibration had been completed, leaving the transported fluid always hypertonic. Yet many epithelia transport isosmotic fluids, and in the case of the gall bladder the experimental error within which the osmolarities of the absorbate and of plasma are identical is less than 2% (Diamond, 1964). It has also been puzzling that in those organs which do form hypertonic secretions, the transported fluid is still hypertonic at the lowest transport rates, when one would expect osmotic equilibration to be most nearly complete.

The experiments described in the previous paper (Tormey and Diamond, 1967) indicated that the route of fluid transport across rabbit gall bladder is by way of long, narrow channels between adjacent epithelial cells, termed the lateral intercellular spaces. There is suggestive evidence that similar lateral spaces could be the route of water transport in the small and large intestine, frog skin, rat proximal tubule, and urinary bladder. In fact, a survey of epithelial ultrastructure shows that long and narrow channels going under a variety of names are a consistent morphological feature of epithelia carrying out fluid transport (Fig. 1). The more familiar examples besides lateral spaces are: the basal infoldings of the ciliary body, salt gland, salivary gland striated duct, choroid plexus, and renal proximal and distal tubule; the bile canaliculi of the liver; and the intracellular canaliculi of the parietal cells of the stomach. In the case of the basal infoldings of the salt gland it has been argued that they constitute the route of fluid transport (Komnick, 1965). (Possibly the microvilli at the luminal surface of the gall bladder and in the brush border of the intestine and proximal tubule should also be included in this list because of their similar geometry, although they differ from the above-mentioned structures in being filled with cytoplasm.) This consistent association between long, narrow channels and fluid transport suggests that there may be some geometrical significance to these structures which results in the observed water-to-solute coupling. That at least some of these structures may serve the same function is made plausible by complementary distribution in the same organ of different species. For example, avian salt gland and lizard distal tubule have basal infoldings, while reptilian salt gland and crocodile distal tubule have lateral spaces (Komnick, 1965; Roberts and Schmidt-Nielsen, 1966; Davis and Schmidt-Nielsen, 1967).

The essential morphological features common to the various subcellular structures mentioned above are that they are long, narrow, fluid-filled spaces

bounded by cell membrane, and generally open at the end facing the solution towards which fluid is being transported but closed at the end facing the solution from which transported material originates (Fig. 2). The crucial physiological consequence of this geometry is that osmotic equilibration will take place progressively along the length of such a structure. Suppose an active transport mechanism deposits solute within the channel, making its contents hypertonic and pulling water in osmotically. Solute will move towards the bathing solution at the open end of the channel as a result of diffusion down

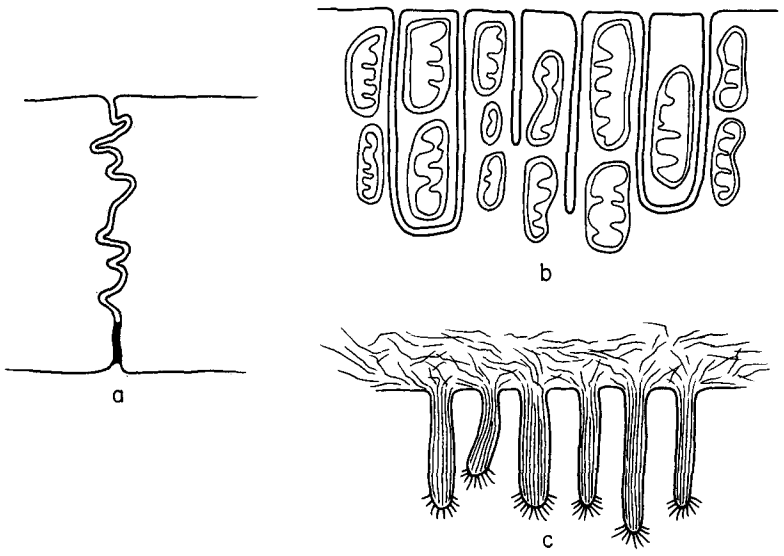

FIGURE 1. Diagrammatic representation of some epithelial structures which may function as standing-gradient flow systems. (*a*) Lateral intercellular space (gallbladder, small intestine, large intestine, rat proximal tubule, lizard salt gland); (*b*) basal infoldings (ciliary body, avian salt gland, salivary gland striated duct, choroid plexus, proximal and distal tubule); (*c*) brush-border microvillus (gall bladder, intestine, proximal tubule, salivary gland duct). Other possible examples are intracellular canaliculi in gastric parietal cells and bile canaliculi in the liver.

its concentration gradient and of being swept along in the water stream. More and more water will enter osmotically along the length of the channel, reducing the osmolarity until the fluid emerging at the open end might be virtually isotonic. In the steady state a standing osmotic gradient would be maintained within the channel by active solute transport, the osmolarity decreasing continuously from the closed towards the open end. From the open end of this flow system a fluid would continually emerge of fixed osmolarity, determined by the parameters of the system.

The basic physical assumption is that the fluid in the channel is unstirred. If this assumption is valid for lateral spaces and basal infoldings, then the

development of standing osmotic gradients in them as outlined here seems inevitable. While there is no question about the existence of circulatory movements and movements of intracellular organelles, the calculated half-times for establishment of the standing gradients are on the order of milliseconds and hence much shorter than the periods of these movements. Thus, it appears improbable that epithelial channels are effectively stirred.

In this paper we shall describe a simplified mathematical model of a standing-gradient flow system, calculate some of its properties, and compare these with the physiological properties of epithelia.

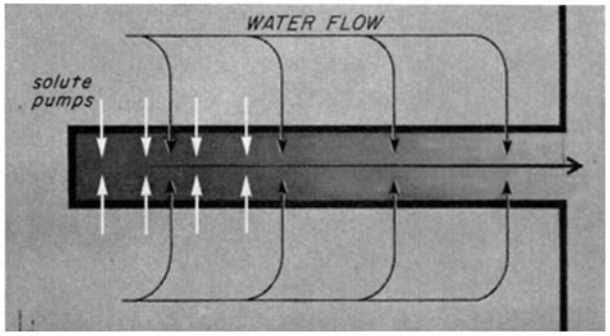

FIGURE 2. Diagram of a standing-gradient flow system, consisting of a long and narrow channel closed at one end. Solute is actively transported into the channel across its walls, making the channel fluid hypertonic. As solute diffuses towards the open mouth, more and more water enters the channel along its length due to the osmotic gradient. In the steady state a standing osmotic gradient would be maintained in the channel by active solute transport, with the osmolarity decreasing progressively from the closed end to the open end. Depending upon values for such parameters as radius, length, and water permeability of the walls, the fluid constantly emerging from the open end may be either isotonic or hypertonic. The depth of shading in the figure indicates the solute concentration

STATEMENT OF THE PROBLEM

The simplest representation of a flow system is a right circular cylindrical channel whose walls are a semipermeable membrane and which is closed at one end and open at the other. The cylinder is oriented along the x-axis, and the closed and open ends are taken as $x = 0$ and $x = L$, respectively.
The independent variables are:

L = the length of the channel
r = the radius
P = the osmotic water permeability of the channel walls, defined as the volume of fluid crossing 1 cm^2 in 1 sec in response to an osmotic gradient of 1 milliosmol per cc or 1 osmol per liter
C_o = the osmolarity of the fluid outside the channels (e.g., the osmolarity

of the intracellular fluid, assumed identical with that of the bathing solutions at the open and closed ends)

D = the diffusion coefficient of the actively transported solute; and

$N(x)$ = the rate of active solute transport across the walls of the channel into its lumen at any height x, defined as milliosmols of solute transported in 1 sec across 1 cm² of channel wall area. (Passive solute movement across the channel walls is assumed to be negligible.)

The dependent variables are:

$C(x)$ = the osmolarity of the fluid in the channel at a height x; and

$v(x)$ = the linear velocity of fluid flow in the channel at height x, taken as positive in the direction $x = 0$ to $x = L$.

The problem is to find the osmolarity of the fluid emerging in the steady state from the open end of the channel. Since in the steady state the rate of solute emergence from the open end must equal the rate of solute transport into the channel integrated over its length, and since water flows out the open end at a rate $\pi r^2 v(L)$, the emergent osmolarity is given by the expression:

$$\frac{2\pi r \int_{x=0}^{x=L} N(x)\, dx}{\pi r^2 v(L)}$$

Consider a disc-shaped segment of the channel extending from $(x - \Delta x)$ to $(x + \Delta x)$. Solute will enter the disc due to active transport across the channel walls at a rate $4\pi r \Delta x N(x)$ milliosmols per sec; due to diffusion along the length of the channel at a rate $2\pi r^2 D \frac{d^2C}{dx^2} \Delta x$; and due to entrainment in the fluid stream at a rate $-2\pi r^2 \Delta x \frac{d}{dx}[v(x)C(x)] = -2\pi r^2 \Delta x \left[C(x) \frac{dv}{dx} + v(x) \frac{dC}{dx} \right]$. In the steady state, when the standing osmotic gradient is established, the net rate of change of solute in the disc must be zero:

$$\frac{2N(x)}{r} + D \frac{d^2C}{dx^2} - C(x) \frac{dv}{dx} - v(x) \frac{dC}{dx} = 0 \qquad (1)$$

Water will enter the disc due to osmosis across the channel walls at a rate $4\pi r P \Delta x[C(x) - C_o]$; and the difference between water flowing into the disc across the plane $(x - \Delta x)$ and leaving across the plane $(x + \Delta x)$ is $-2\pi r^2 \frac{dv}{dx} \Delta x$.

In the steady state the net rate of change of water in the disc must be zero:

$$\frac{dv}{dx} = \frac{2P}{r}[C(x) - C_o] \qquad (2)$$

Rearranging equation (2):

$$C(x) = \frac{r}{2P}\frac{dv}{dx} + C_o \tag{3}$$

Substituting equation (3) into equation (1):

$$N(x) + \frac{Dr^2}{4P}\frac{d^3v}{dx^3} - \frac{r^2v}{4P}\frac{d^2v}{dx^2} - \frac{C_0r}{2}\frac{dv}{dx} - \frac{r^2}{4P}\left(\frac{dv}{dx}\right)^2 = 0$$

There are three boundary conditions:

1. No solute diffuses across the closed end of the channel; i.e., at $x = 0$, $\frac{dC}{dx} = 0 = \frac{d^2v}{dx^2}$.
2. No water moves across the closed end; i.e., at $x = 0$, $v = 0$. One could also permit fluxes across the closed end, but this would merely complicate the mathematics without altering the outcome as long as the channel is narrow.
3. At $x = L$, $C(x) = C_o$, and therefore $\frac{dv}{dx} = 0$. This condition is automatically fulfilled by an isotonically transporting system and should also be valid for an anisotonically transporting system provided the vascular supply is adequate.

Since we were unable to find an analytical solution to this problem, it was evaluated numerically as described in the Methods section.

Implicit in this treatment are several assumptions which bear discussion:

1. That the channel wall is impermeable to solute, so that solute will produce the full van't Hoff osmotic water flow (i.e., the solute reflection coefficient σ is unity) and back-diffusion of solute across the channel wall will be negligible. This assumption should be approximately correct in most cases, since measurements of σ's in epithelia for actively transported solutes have generally yielded values close to 1. Deviations from this assumption (i.e., values of σ less than 1, and passive back-diffusion of solute not negligible compared to the active solute transport rate) can be shown to be equivalent in the first approximation to a decrease in the value of $N(x)$.

2. That the hydrostatic pressures within the channel are much less than RT (gas constant and absolute temperature) times the osmolarity differences across the channel walls, so that back-loss of water across the channel walls by filtration may be neglected. There is no question that some hydrostatic pressure is developed in the channels, as evidenced by the dilatation of lateral intercellular spaces during transport. However, calculation from the observed channel dimensions and water flows shows that these pressures should be of the order of 1 cm H_2O or less (≤ 0.001 atmosphere), and this is in fact negligible

compared to the expected osmotic driving forces across the channel of approximately 1 to 5 atmospheres. It is important to appreciate that as long as channel pressures are negligible compared to osmotic driving forces, a hydraulic resistance beyond the mouth of the channel (e.g., due to the connective tissue or basement membrane) simply raises the absolute hydrostatic pressure level in the channel and has no direct effect on the emergent osmolarity, since concentration profiles, diffusion rates, and osmotic influxes in the channel are unaltered.

3. That radial effects may be neglected; i.e., that C and v are functions only of x and not of radial position in the channel. With channel diameters of 200 A to 1 μ, half-times for radial diffusion equilibrium will range from about 0.1 to 250 μsec, so that radial variations in C may safely be neglected. v would surely be greater along the central axis of the channel than at the walls and would in fact be zero at the walls if Poiseuille flow obtained. However, in channels narrower than about 0.1 μ Poiseulle's law breaks down, and "sliding" of fluid along the walls makes an appreciable contribution to the total flow, reducing the radial variation in v (Derjaguin, 1965). Whatever the exact radial variation in v, it would affect the results if it could set up a radial variation in C, but this is precluded by the rapidity of radial diffusion equilibrium in channels of the sizes encountered biologically. Hence $v(x)$ in equations 1–3 should be regarded as a mean value with respect to radius.

4. The geometries of the biological structures hypothesized to be standing-gradient flow systems are, of course, not right circular cylinders but in general something more complex. Nevertheless, if the basic principles of standing gradients and progressive osmotic equilibration apply, the qualitative conclusions deduced from the cylindrical idealization should still be valid, and alterations would only be in quantitative details. For example, the equations appropriate to two infinite parallel planes (a closer approximation to basal infoldings), or to a thin cylindrical ring (a closer approximation to lateral spaces), can be shown to be identical in form to those for a cylinder evaluated in this paper.

METHODS

Mathematical Techniques Equations (1) and (2) can be rewritten as a set of simultaneous first-order ordinary differential equations:

$$\frac{dv}{dx} = \frac{2P}{r}[C(x) - C_o]$$

where $v = 0$ at $x = 0$;

$$\frac{dC}{dx} = B$$

where $C = C_o$ at $x = L$; and

$$\frac{dB}{dx} = \left(C\frac{dv}{dx} + vB - \frac{2N}{r}\right) \Big/ D$$

where $B = 0$ at $x = 0$.

Equations 4–6 were integrated numerically by an iterative procedure based on the second-order Runge-Kutta formulae (Ralston and Wilf, 1960) and the so-called "method of false position" (Kunz, 1957). For two arbitrary choices of $C(0)$, the concentration at $x = 0$, Runge-Kutta integrations were performed over the range $0 < x < L$ using 500 equal steps in x. This gave two values of $C(L)$ from which an estimate of the value of $C(0)$ corresponding to $C(L) = C_o$ could be obtained by linear interpolation. The integration and interpolation were then repeated using the improved estimates of $C(0)$ until integration yielded a value of $C(L)$ which differed by less than some predetermined limit, usually ± 0.01 %, from C_o.

Some restrictions on the initial choices of $C(0)$ can be deduced from the equations. As long as N is positive, $C(0)$ must be greater than C_o. On the other hand, $C(0)$ must be less than $\left(C_o + \sqrt{C_o^2 + \frac{4N}{P}}\right) \Big/ 2$. This follows from equations 4–6 and in particular from the fact that if both $\frac{dC}{dx}$ and $\frac{d^2C}{dx^2} = \frac{dB}{dx}$ are simultaneously positive, C will not approach C_o but will become indefinitely large. However, choosing $C(0)$ less than this value only guarantees that the derivatives will not both be positive at $x = 0$, and in general this condition can still occur at some point in the integration for smaller values of $C(0)$. The problem is complicated by the fact that the relation between an estimated $C(0)$ and the resulting calculated $C(L)$ becomes quite nonlinear for larger values of $C(0)$, so that extrapolation upward from lower values is usually fruitless. For these reasons it was often necessary to try a number of values of $C(0)$ in order to select two for which the iterative procedure would converge.

The integrations were performed on the IBM 7094 computer using programs written in the FORTRAN language.

Justification of Numerical Values Chosen In selecting numerical values for model parameters, we have attempted to cover the range of physiological values for each parameter in epithelia, reasoning as follows:

Channel Radius (r) At the lower extreme, basal infoldings (e.g., in kidney tubule and ciliary epithelium), and the lateral channels of the gall bladder when collapsed), are about 200 A wide. When distended, the lateral channels of the gall bladder average 0.9 μ in diameter and range up to about 2 μ. The range of r was therefore taken as 0.01 to 1 μ.

Channel Length (L) A range of $L = 4$ to 200 μ was chosen to encompass the lengths of most basal infoldings and lateral spaces in epithelia. We selected the apparently high upper limit of 200 μ to allow for increases in effective channel length over their nominal values due to tortuosity. For example, the lateral channels of rabbit gall bladder average 32 μ in length when measured in a straight line, but the

effective value may be several times higher when interdigitating cytoplasmic projections increase the tortuosity. This range would not, however, include the lengths of apical microvilli (one-half to several microns).

Solute Diffusion Coefficient (D) The most rapidly diffusing solute that is actively transported in osmotically significant quantities would be HCl in the mammalian and avian stomach (D_{HCl} about 4×10^{-5} cm^2 per sec at 36–42°C in free solution), while the slowest would be bile salts secreted by the liver (D probably 1 to 3×10^{-6} cm^2 per sec in free solution). The range of D was therefore taken as 1×10^{-6} to 5×10^{-5} cm^2 per sec. It is possible that still lower values occur biologically, since under certain circumstances actual diffusion coefficients may be lower than free solution values (p. 2076).

Solute Transport Rate (N) The highest recorded transport rates are for mammalian gall bladder and proximal tubule in vivo, approximately 0.5×10^{-5} to 1.5×10^{-5} milliosmols per sec per cm^2 of apparent total epithelial surface area. If one calculates the increase in surface area due to microscopic folding and the fraction of the total area occupied by lateral intercellular spaces, and if one assumes that the transport mechanism is distributed uniformly over the lengths of the spaces, then one arrives at N = approximately 10^{-6} milliosmols per sec per cm^2 channel wall area. However, solute pumps may not be uniformly distributed, and if, to take an extreme case, all transport is confined to the bottom tenth of the channel, N would be 10^{-5} milliosmols per cm^2, sec. At the other extreme, the transport rate may be indefinitely low, and in practice we calculated a range of N from 10^{-5} down to 10^{-10} milliosmols per cm^2, sec.

Osmotic Water Permeability (P) The following are the values obtained in representative epithelia by measuring water flow across the whole epithelium in response to an external osmotic gradient: toad skin, 3.5×10^{-6} cm per sec, Osm (Bentley, 1961); frog skin, 6×10^{-6} (Dainty and House, 1966); frog stomach, 2×10^{-5} (Durbin, Frank, and Solomon, 1956); *Necturus* kidney proximal tubule, 3.8×10^{-5} (Whittembury, Oken, Windhager, and Solomon, 1959); rabbit gall bladder, 4.4×10^{-5} (Diamond, 1964); fish gall bladder, 1.2×10^{-4} (Diamond, 1962); and rat small intestine, 1.7×10^{-4} (Smyth and Wright, 1966). The regions of an epithelium specialized for transport may well have different permeabilities, but these values may at least be considered a guide, and we therefore employed a range of P from 1.0×10^{-6} to 2.0×10^{-4} cm per sec, Osm.

RESULTS

Concentration and Velocity Profiles Figs. 3 and 4 reproduce concentration and velocity profiles in the channel calculated for four sets of values of the model parameters. Under all circumstances the solute concentration decreases and the velocity of flow increases continually from the closed end to the mouth of the channel, but the exact forms of the profiles depend upon the conditions. In general, when diffusion is much more important than water flow in carrying solute out the mouth of the channel, the solute concentration will fall off

nearly linearly from the end of the transport site to the mouth. Any factor that increases the relative importance of water flow makes the concentration profile more nonlinear. For example, decreasing the osmotic permeability of the channel walls without changing the solute transport rate yields a more linear profile (curve 2 vs. curve 4, Fig. 3) by decreasing water flow. Flatter concen-

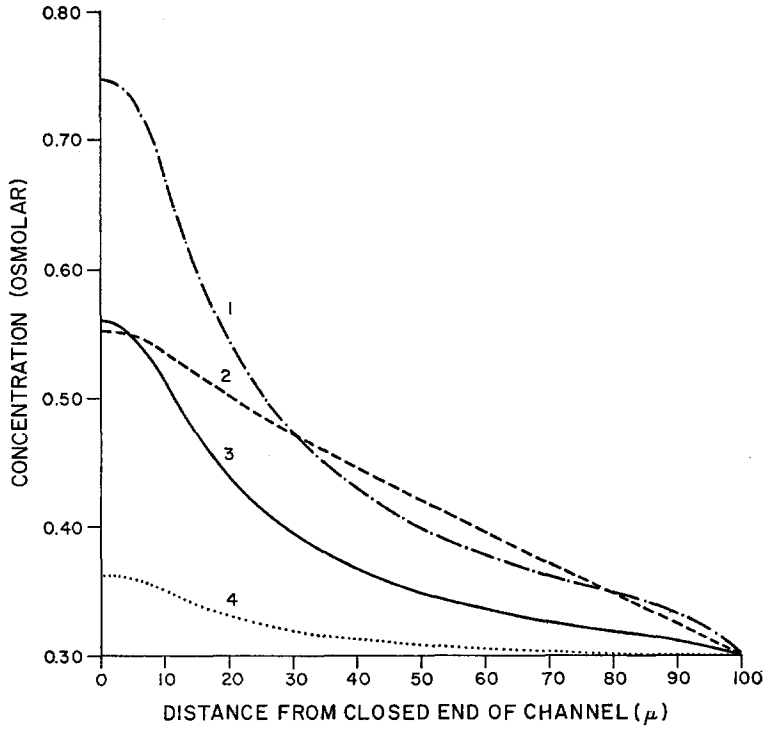

FIGURE 3. Examples of concentration profiles in a standing-gradient flow system. The solute concentration in the channel in the steady state (ordinate) is plotted against x, the linear distance from the closed end of the channel (abscissa). L was held fixed at 100 μ, r at 0.05 μ, C at 0.3 OSM, and D at 10^{-5} cm^2 per sec. N was held at 10^{-5} (curve 1), 5×10^{-6} (curve 3), or 10^{-6} (curves 2 and 4) milliosmols per cm^2, sec for $0 < x < 10\mu$, and at zero for $x > 10$ μ. P was held at 2×10^{-5} (curves 1, 3, and 4) or 1×10^{-6} (curve 2) cm per sec, OSM. The corresponding calculated concentrations of the emergent fluid were 0.342 (curve 1), 0.803 (curve 2), 0.318 (curve 3), and 0.304 (curve 4) OSM.

tration profiles are obtained if solute transport extends from the closed end of the channel over a greater fraction of its length.

It is important to realize that the concentration of the emergent fluid is in general *not* equal to the standing concentration of solute at the mouth of the channel ($C(L)$), because solute can leave the channel by diffusion as well as by being swept along with the water flow. Since $C(L)$ always equals the bathing solution concentration C_o as a boundary condition, the necessary condition

for the emergent fluid to have this same concentration (i.e., be isotonic) is that $\frac{dC}{dx} = 0$ at $x = L$; i.e., that the concentration profile near the mouth of the channel be flat because osmotic equilibration is virtually complete.

Effect of Channel Length (L) Fig. 5 shows the effect of variations in channel length upon the emergent concentration, all other parameters being held constant. It is apparent that the emergent fluid becomes less hypertonic and asymptotically approaches isotonicity, the longer the channel. This is to be expected as a result of the longer diffusion pathway and the increased channel length over which osmotic equilibration can take place.

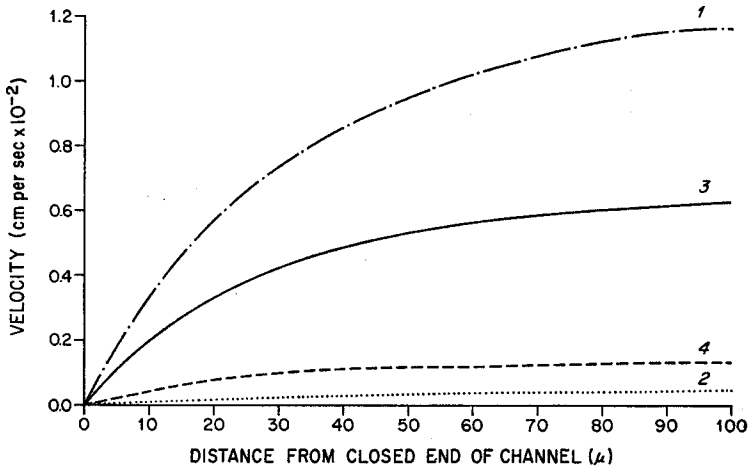

FIGURE 4. Velocity profiles in a standing-gradient flow system, corresponding to the concentration profiles of Fig. 3. The linear velocity of water flow in the channel in the steady state (ordinate) is plotted against x, the linear distance from the closed end of the channel (abscissa). Symbols and values as in Fig. 3.

Effect of Channel Radius (r) Fig. 6 illustrates the effect of variations in channel radius upon the emergent concentration. The area of channel wall, of course, increases in proportion to the radius, and P (osmotic water permeability per unit area) is assumed constant, so that the total water permeability of the channel increases with the radius. For the purposes of this calculation the total amount of solute transported into the channel is held constant, so that proportionally higher transport rates per unit area were chosen with decreasing radii. It is apparent from Fig. 6 that as the channel becomes narrower, the emergent fluid becomes less hypertonic and approaches isotonicity asymptotically. The intuitive explanation is that the area of the channel varies as the first power of the radius but the volume as the second power. Thus, as the radius of the channel decreases, the same amount of solute is being transported

into a smaller volume, so that its concentration is higher and it will pull in more water osmotically.

If the radius is varied while maintaining the total water permeability of the channel constant by choosing higher P's at lower r's, the emergent fluid still is found to approach isotonicity with decreasing radius.

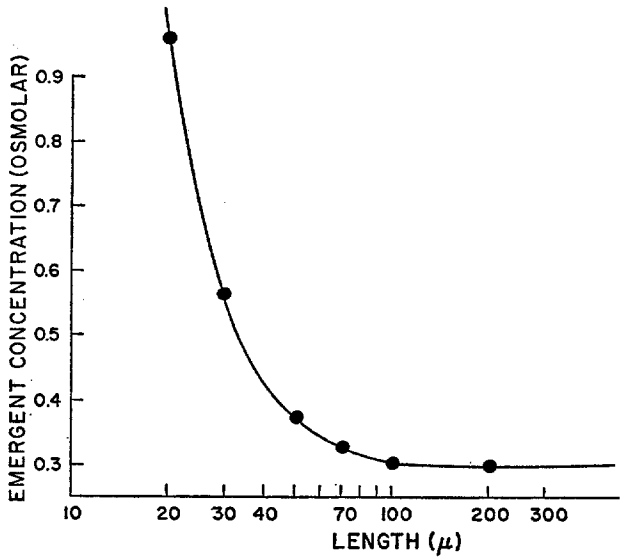

FIGURE 5. The effect of varying channel length upon the osmolarity of fluid produced by a standing-gradient flow system. The parameters of the system other than length were held fixed at the following values: $P = 2 \times 10^{-5}$ cm per sec, OSM; $r = 0.05$ μ; $D = 10^{-5}$ cm^2 per sec; $C_o = 0.3$ OSM; $N = 10^{-6}$ milliosmols per cm^2, sec from $x = 0$ to $x = 10$ μ, $N = 0$ for $x > 10$ μ. The abscissa is channel length plotted on a logarithmic scale.

Effect of Water Permeability (P) Fig. 7 shows that when other parameters are held constant, the emergent concentration becomes less hypertonic and approaches isotonicity asymptotically with increasing values of P, the water permeability per unit area. The same conclusion follows from Figs. 8–10.

Effect of Solute Transport Rate (N) When the other parameters of the system are held constant, the osmolarity of the emergent fluid decreases with decreasing N at very high rates and approaches asymptotically a limiting value (Fig. 8). This value may be either hypertonic or virtually isotonic depending upon the values of L, P, and r, and it is a characteristic of the system. For example (Fig. 8), when L and r are held constant at 100 μ and 0.05 μ, respectively, the limiting osmolarity is isotonic (0.3 OSM) when the water permeability P equals 2×10^{-5} cm per sec, OSM; hypertonic (about 0.495 OSM) when P is reduced to 2×10^{-6}; and still more hypertonic (about 0.745 OSM) when P is reduced to 1×10^{-6}.

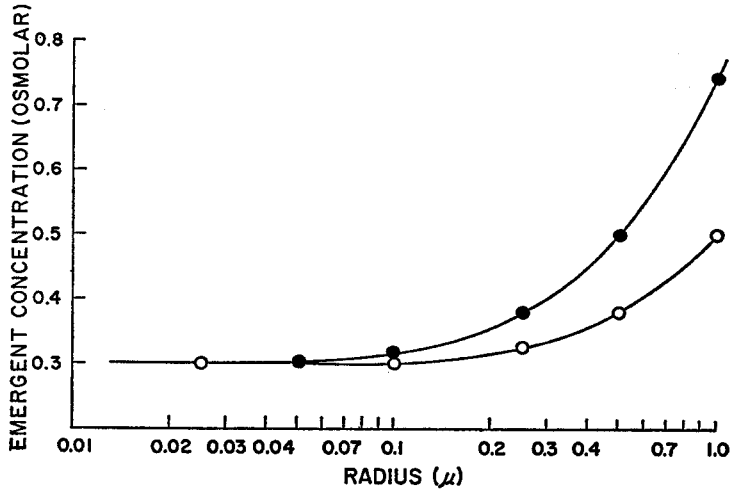

FIGURE 6. The effect of varying channel radius upon the osmolarity of fluid produced by a standing-gradient flow system. L was held fixed at 100 μ, C_o at 0.3 OSM, and D at 10^{-5} cm^2 per sec. P was held fixed at 2×10^{-5} (upper curve, solid circles) or at 4×10^{-5} (lower curve, open circles) cm per sec, OSM. From $x = 0$ to $x = 10$ μ the transport rate per unit channel length was held fixed at $\pi \times 10^{-11}$ milliosmols per cm, sec, independent of variations in r, by choosing N (the transport rate per unit wall area) as $\frac{\pi \times 10^{-11}}{2 \pi r}$ milliosmols per cm^2, sec. At $x > 10$ μ, N was always zero. The abscissa is radius plotted on a logarithmic scale.

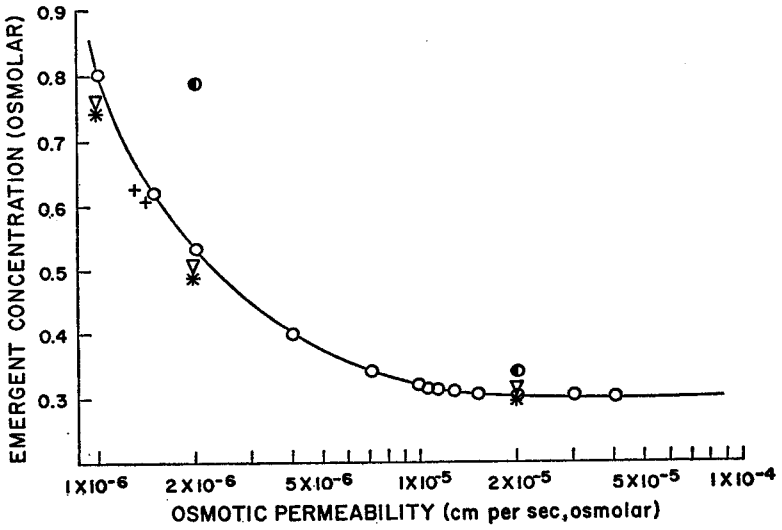

FIGURE 7. The effect of varying channel water permeability upon the osmolarity of fluid produced by a standing-gradient flow system. L was held fixed at 100 μ, r at 0.05 μ, C_o at 0.3 OSM, and D at 10^{-5} cm^2 per sec. N was held at 10^{-5} (◐), 10^{-6} (○), 10^{-7} (▽), 10^{-8} (+), or 10^{-9} (×) milliosmols per cm^2, sec. The abscissa is osmotic water permeability plotted on a logarithmic scale.

These interrelations between the effects of transport rate and permeability are also illustrated in Fig. 7. At any given value of P the transported osmolarity is virtually independent of the transport rate for values of N below about 10^{-7} milliosmols per cm^2, sec, and the value of this limiting osmolarity increases with decreasing P. Increasing the transport rate to 10^{-6} makes the transported fluid slightly more hypertonic, and increasing the transport rate by another factor of 10 yields a transported fluid which is much more hypertonic at any given value of P.

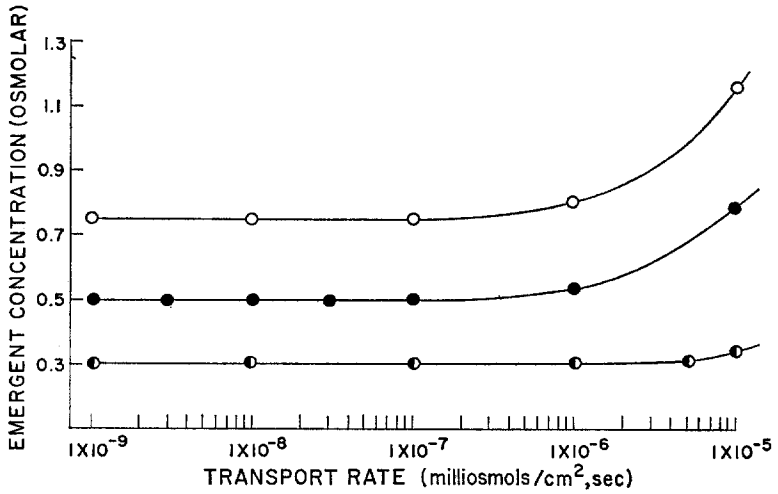

FIGURE 8. The effect of varying solute transport rate upon the osmolarity of fluid produced by a standing-gradient flow system. L was held fixed at 100 μ, r at 0.05 μ, C_o at 0.3 OSM, and D at 10^{-5} cm^2 per sec. P was held at 2×10^{-5} (◐), 2×10^{-6} (●), or 1×10^{-6} (○) cm per sec, OSM. The abscissa is transport rate plotted on a logarithmic scale. This value of transport rate holds in the range $0 < x < 10$ μ, and the rate is zero for $x > 10$ μ.

The possible physiological significance of the transported osmolarity remaining virtually constant over a wide range of transport rates is considered in the Discussion section.

Effect of Site of Solute Transport In Figs. 3–8 the active solute transport was confined to the bottom tenth of the channel. The effect of varying the distance from the closed end of the channel over which solute input takes place, while maintaining the same total rate of solute input for the whole channel, is considered in Fig. 9. The emergent concentration is most nearly isotonic when solute input is confined to the closed end of the channel, and becomes progressively more and more hypertonic as transport is spread over a greater fraction of the channel length towards the open end. The reason is that the osmotic inflow of water decreases as the length of channel over which

osmotic equilibration can occur decreases, and diffusion becomes more important as the diffusion pathway to the outside shortens. The extent of this hypertonicity depends upon the other parameters of the system (L, P, and r). For example, at the lower value of the water permeability ($P = 2 \times 10^{-5}$ cm

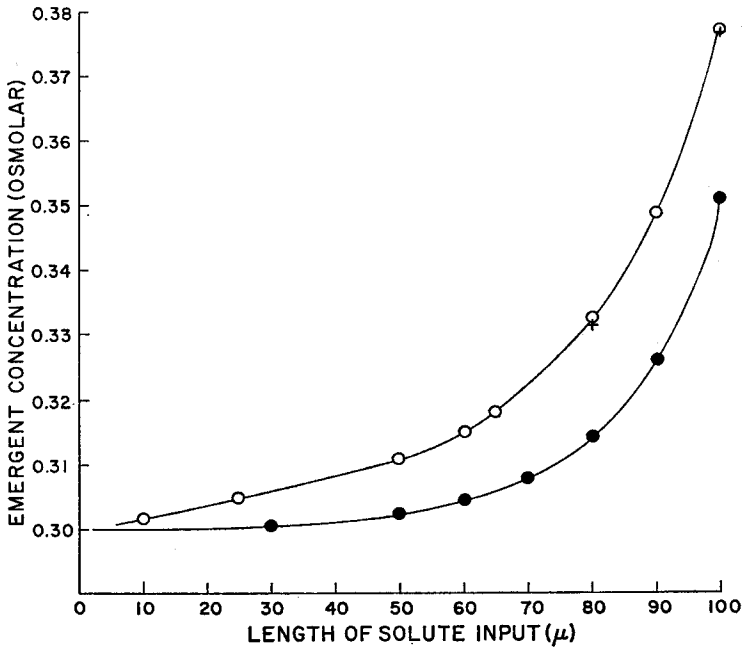

FIGURE 9. The effect of solute transport site upon the osmolarity of fluid produced by a standing-gradient flow system. L was held fixed at 100 μ, r at 0.05 μ, C_o at 0.3 OSM, and D at 10^{-5} cm^2 per sec. P was held at 2×10^{-5} (○ and +) or 4×10^{-5} (●) cm per sec, OSM. A given solute transport rate (N) held over a range of x from zero out to the value given on the abscissa, and N was zero for x greater than this value. The transport rate for the whole channel was held fixed at $(2\pi rL)$ (10^{-8}) milliosmols per sec, by choosing N (transport rate per unit wall area) as (100) (10^{-8}) divided by the length of solute input, in milliosmols per cm^2, sec (○ and ●). For example, when transport took place into the whole length of the channel (input length = 100 μ), N was taken as 10^{-8} milliosmols per cm^2, sec, and when transport took place only into the bottom tenth of the channel (input length = 10 μ), N was taken as 10^{-7} milliosmols per cm^2, sec. In the two points marked by crosses N was ten times lower; i.e., the transport rate for the whole channel was held fixed at $(2\pi rL)$ (10^{-9}) milliosmols per sec.

per sec, OSM) the transported fluid is 1% hypertonic (i.e., 0.303 OSM) when solute transport is spread over the bottom 16% of the channel, and 5% hypertonic (0.315 OSM) when transport extends over 60% of the channel length. When the water permeability is doubled ($P = 4 \times 10^{-5}$), transport can occur over much more of the channel before these degrees of hypertonicity are reached: the emergent fluid is 1% hypertonic when transport extends over

53% of the channel, and 5% hypertonic when transport extends over 81%. Fig. 9 also shows (compare crosses and open circles) that even when transport is spread over 80% or the entirety of the channel length, the transported osmolarity is still relatively independent of the solute transport rate, as explained in the preceding section.

Effect of Solute Diffusion Coefficient (D) There is considerable experimental evidence that the properties of water in channels narrower than about 10^{-5} cm (1000 A) begin to deviate significantly from the properties of bulk water,

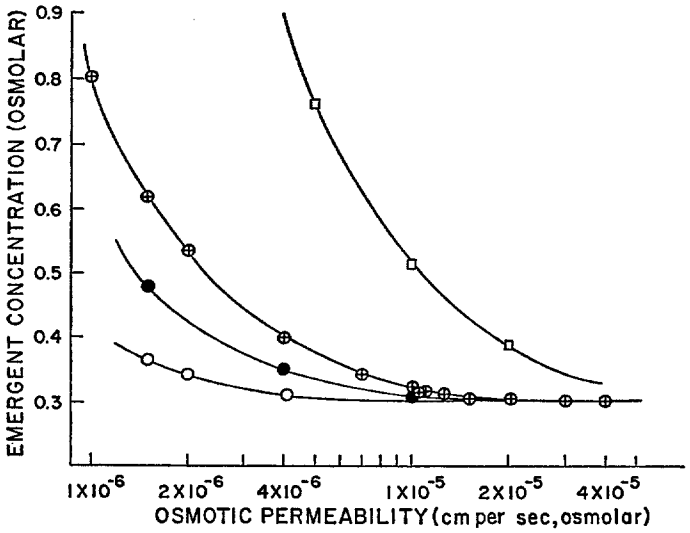

FIGURE 10. The effect of solute diffusion coefficient upon the osmolarity of fluid produced by a standing-gradient flow system. L was held fixed at 100 μ, r at 0.05 μ, C_o at 0.3 OSM, and N at 10^{-6} milliosmols per cm², sec for the range $0 < x < 10$ μ and zero for $x > 10$ μ. The abscissa is the osmotic water permeability plotted on a logarithmic scale. D was taken as 10^{-6} (○), 5×10^{-6} (●), 10^{-5} (⊕), or 5×10^{-5} (□) cm² per sec.

pointing to a more ice-like organization of the water structure (Henniker, 1949; Derjaguin, 1965). Examples of these anomalous properties in narrow channels are: increased viscosity; breakdown of Poiseuille's law, and dependence of flow on powers of the channel radius lower than 4; increased specific heat; and change in the thermal expansion of water such that there is no maximum density at 4°C but instead a linear dependence of volume upon temperature. In most cases these altered properties of liquid water in small channels are intermediate between the properties of ice and of bulk water. Presumably, then, the diffusion coefficients of solutes in narrow channels would be less than in bulk water. Since the dimensions of the channels postulated as pathways of epithelial water transport (r = 100 A–5000 A) often

fall into the range where these anomalous properties of water appear, it seemed desirable to examine the behavior of the standing-gradient model as a function of solute diffusion coefficient. In addition, the appropriate value of D to be used will vary among different organs, depending upon the solute being actively transported and the temperature.

Fig. 10 shows that the emergent fluid becomes less hypertonic (approaches closer to isotonicity) as the solute diffusion coefficient is lowered. The explanation is that solute will diffuse out of the channels more slowly, so that osmotic equilibration will proceed further, and the osmotic water flow itself will become more important in determining the exit of solute from the channels.

DISCUSSION

The intuitive meaning of Figs. 5–10 may be expressed as follows. Two forces are responsible for carrying solute out the open mouth of the system: the diffusion of solute down its concentration gradient, and the sweeping effect of water flow upon solute. Any factor that increases the relative importance of diffusion will make the emergent fluid more hypertonic, while factors increasing the relative importance of water flow are associated with a more nearly isotonic emergent fluid. For example, diffusion proceeds more slowly in a long channel, or when the solute transport is concentrated at the closed end of the channel, or when the diffusion coefficient of solute is reduced. Under these circumstances it is the osmotic water flow itself, set up by active solute transport, that determines the rate of solute egress, and solute therefore cannot escape until osmotic equilibration to virtual isotonicity has taken place (Figs. 5, 9, and 10). Similarly, a decrease in channel radius means that a given rate of solute transport will produce higher osmotic concentrations within the channel. Thus, either a decrease in radius or an increase in water permeability, both of which cause increased rates of osmosis, is associated with closer approaches to isotonicity (Figs. 6 and 7). At the opposite extreme, in a very short channel diffusion to the outside will be rapid, and little water will have followed the solute osmotically by the time it has diffused to the channel mouth; i.e., the emergent fluid will be quite hypertonic.

No consistent relation exists between the emergent concentration and $C(0)$, the standing concentration at the closed end of the channel. A decrease in radius, increase in length, decrease in diffusion coefficient, or decrease in the length of solute input all make the emergent concentration more nearly isotonic while increasing $C(0)$; an increase in permeability makes the emergent concentration more isotonic while decreasing $C(0)$; and an increase in solute transport rate has little effect on the emergent concentration while increasing $C(0)$.

It should also be reemphasized that since the emergent concentration

depends upon several different parameters, this concentration cannot be predicted from the value of one parameter alone. For example, with the particular values of L, P, N, and D chosen in Fig. 6, the transported fluid becomes noticeably hypertonic at radii above about 0.3 μ. This does not mean, however, that isotonically transporting epithelia with channels wider than this value could not be functioning as standing-gradient systems: the emergent concentration could be isotonic at much wider radii if, for example, P were higher or D lower than the values used in Fig. 6. This same point has also been discussed with respect to the site of solute transport (p. 2074).

In considering the possible biological significance of standing gradients, the following points may be noted:

1. The emergent osmolarities calculated in Figs. 5–10 for channels of the dimensions observed in epithelia, with permeabilities and transport rates similar to those measured in epithelia, fall generally in the range of epithelial absorbates and secretions (isotonic up to a few times isotonic). In other words, the solute-water coupling and transported osmolarities characteristic of epithelia may be regarded as an automatic consequence of epithelial ultrastructure.

2. The intuitive expectation that a standing-gradient system can yield a fluid that is isotonic within any arbitrary degree of accuracy is confirmed by calculation. In the past, much experimental effort has gone into attempts to detect slight osmotic pressure differences between "isotonic" secreted fluids and plasma, that could serve as driving forces for water flow during secretion. These efforts have generally yielded either the conclusion that the transported fluid is isotonic within experimental error, or, if it is in fact slightly hypertonic, that this driving force is insufficient to cause the observed rates of water flow when measurements of the water permeability of the epithelium are taken into account (Auricchio and Bárány, 1959; Diamond, 1964). This finding is readily explicable in terms of the standing-gradient hypothesis, on the basis of which no osmotic pressure difference between plasma and the final transported fluid need exist, since the osmotic gradient responsible for fluid movement would exist entirely within the lateral spaces and basal infoldings.

3. In regard to epithelia forming hypertonic absorbates or secretions, it has generally been expected that the transported fluid would become progressively less hypertonic as the transport rate was lowered, on the grounds that the time available for osmotic equilibration would then be greater. Experimentally, however, absorption from such structures as the distal tubule and sweat and salivary gland duct is still hypertonic even at low transport rates. The best quantitative evidence comes from the avian salt gland, which has been shown to produce a hypertonic secretion whose osmolarity is virtually independent of transport rate (Schmidt-Nielsen, 1960). Similarly, Davis and Schmidt-Nielsen (1967) found that the osmolarity of the hypertonic absorbate formed by

crocodile distal tubule is practically rate-independent. These experimental observations accord with predictions of the standing-gradient model: if an epithelial channel has evolved with a length, radius, and permeability such that the emergent fluid is hypertonic, then this degree of hypertonicity will be maintained as the transport rate is decreased indefinitely (Figs. 7 and 8).

4. Figs. 7 and 8 also indicate that a relatively modest increase in permeability, without changes in other parameters, can convert the output of a standing-gradient system from markedly hypertonic to isotonic, suggesting an analogy for the action of antidiuretic hormone upon reabsorption by the distal tubule.

5. In a few epithelia one finds cells with channels which appear to be oriented in the opposite direction; i.e., with the closed end in the direction of net fluid movement. For instance, the ependymal cells of the choroid plexus resemble absorptive cells morphologically (e.g., in the presence of a brush border and basal infoldings), but the net direction of flow of cerebrospinal fluid is secretory. If one evaluates equations 1–3 for negative values of N, i.e. for solute uptake out of the channels rather than secretion into them, one finds that the channel contents become increasingly hypotonic towards the closed end. The result is water uptake out of the channels coupled to solute uptake, so that long and narrow channels can function in either direction. The basal infoldings of the choroid plexus could thus accomplish isotonic fluid transport from blood to cells, as required physiologically.

6. While the dimensions of basal infoldings and lateral intercellular spaces in epithelia are such that they may plausibly be considered to operate as standing-gradient systems, the extension of the model to the microvilli of brush borders is much more speculative. As discussed in the previous paper, the available evidence makes it likely, though it does not prove, that the solute and water emerging from the lateral spaces of the gall bladder first cross the luminal cell membrane, where the details of solute transport are still obscure. One must then account for isotonic water-to-solute coupling not only at the lateral membrane, where the lateral spaces would provide the answer, but also at the luminal membrane. It is tempting to attribute coupling at the luminal membrane to standing gradients in the microvilli, and in fact there are no other luminal structures that would suggest a plausible alternative hypothesis. Microvilli are found not only at the luminal surface in gall bladder epithelium, which carries out no other significant function except coupled salt and water transport, but also in other absorptive tissues (e.g., gut and proximal tubule). The chief objection to this circumstantial line of reasoning is that microvilli are considerably shorter (0.5–4 μ) than the other epithelial structures under consideration as standing-gradient systems. All other things being equal, completeness of equilibration decreases with decreasing channel length (Fig. 5), and one may well doubt whether microvilli are sufficiently long to account for

isotonic fluids. Of course, a short length might be offset by some other factor, but available estimates make it unlikely that the radius of the microvilli is small enough, or the permeability high enough, to help. More promising is the possibility that the diffusion coefficient of NaCl in the microvilli might be drastically reduced below the free-solution value, due to the close packing of fine fibers in their core and in the terminal web (Tormey and Diamond, 1967). A reduction in D would promote osmotic equilibration markedly (cf. Fig. 10), but until there is evidence for such an effect, both the hypothesis of standing gradients in microvilli and the structural basis of water transport at the luminal membrane must remain uncertain.

That solute transport into a restricted space can give rise to water fluxes between identical external solutions was first demonstrated experimentally by Curran and MacIntosh (1962) in a model system consisting of three compartments in series, and this double-membrane model was analyzed mathematically by Patlak, Goldstein, and Hoffman (1963). The standing-gradient model discussed here retains the basic concept of equilibration in a restricted space from the Curran-Patlak analysis but differs in several features suggested by the more recent anatomical evidence. These are: that the folded geometry of the transporting structures may be important in permitting sequential equilibration along a standing osmotic gradient; that the assumption of perfect stirring no longer seems physically realistic in the light of this geometry; and that equilibration may depend upon only a single membrane of appropriate shape, since the connective tissue and basement membrane apparently do not represent a functionally significant second membrane (Tormey and Diamond, 1967). The restriction to solute diffusion thus arises simply from the observed length of the channel rather than from an assumed second membrane, though the constricted mouths of gall bladder lateral spaces require quantitative evaluation as a possible contributing factor. The incorporation of these features makes it possible to obviate the necessity in a well stirred system for assuming epithelial water permeabilities much higher than those actually measured (Auricchio and Bárány, 1959; Diamond, 1964; Whitlock and Wheeler, 1964), which has been one of the basic dilemmas in explaining isotonic fluid transport. These features also lead to the distinctive relations between osmolarity and transport rate predicted in Figs. 7 and 8 and observed experimentally (cf. p. 2078).

Two kinds of observations may assist in determining whether standing osmotic gradients actually are set up in epithelia. The less direct of these is suggested by Fig. 9, which shows that the emergent fluid is more likely to be isotonic when the transport mechanism is concentrated towards the closed end of the channel. Localization of the transport mechanism is not a conclusive test of the hypothesis, since a higher water permeability or narrower radius could still preserve isotonicity even if the solute "pump" were found to be

spread over virtually the entire length of the channel. However, the converse finding—preferential localization of solute pumps, e.g. towards the closed (luminal) end of lateral intercellular channels in the gall bladder and intestine—would certainly be suggestive that standing gradients were being set up. Some indication that this may be the case is provided by the distribution of mitochondria in rabbit gall bladder, which were shown to be present in highest concentration at the luminal end of the cell (Tormey and Diamond, 1967). In principle, the localization of transport sites might also perhaps be inferred from the distribution of ATPase, and a histochemical method involving precipitation of released inorganic phosphate by lead has been widely used with this aim and tacitly assumed to demonstrate "pump ATPase." However, critical evidence that ATPase so localized bears any relation to transport is wanting. For example, Tormey (1966) found that the ATPase which is histochemically demonstrable on the basal folds of the ciliary epithelium possesses none of the properties which would be expected of Na-K–activated (pump) ATPase: viz., it is not activated by Na and K, it is not inhibited by ouabain, and it is activated by Ca. Kaye, Wheeler, Whitlock, and Lane (1966) reported ATPase activity along the entire length of the lateral intercellular spaces of rabbit gall bladder, but Tormey (personal communication) did not find this activity to be activated by NaCl or inhibited by ouabain; it therefore does not seem to be related to the NaCl pump which drives water transport in this organ and which may be inhibited by the lead-precipitating reagent.

The alternative would be to localize the actively transported solutes themselves; e.g., to determine whether the concentrations of Na and Cl in the lateral spaces of the gall bladder decrease from the tight junction to the basement membrane. The technical problem will be to devise a localization procedure during which solute is not free to diffuse and dissipate the gradient. For example, attempts at sodium localization in rabbit gall bladder have been carried out by pyroantimonate precipitation (Kaye, Wheeler, Whitlock, and Lane, 1966), but this technique is not suitable for assessing standing gradients due to the continuing diffusion of solutes that can occur during fixation. Because of unstirred layers adjacent to the epithelium, half-times for diffusion to the basal end of the epithelial cells of rabbit gall bladder are on the order of half a minute and several minutes for substances added to the mucosal and serosal bathing solutions, respectively. These half-times vary inversely as the diffusion coefficient of the substance. If as much as 1 sec elapses between arrival of osmium (cessation of transport) and arrival of pyroantimonate (precipitation of sodium), half of the sodium will have diffused 30 μ, so that detection of any concentration differences within the lateral spaces would be manifestly impossible. The solution to this dilemma will probably have to await the development of methods for solute localization in quick-frozen tissue.

This work was supported in part by grants from the Public Health Service (GM 14772) and Advanced Research Projects Agency (SD 265), and was carried out during tenures of Junior Fellowships from the Society of Fellows, Harvard University, by both of us.

Received for publication 16 January 1967.

REFERENCES

AURICCHIO, G., and E. H. BÁRÁNY. 1959. On the role of osmotic water transport in the secretion of the aqueous humour. *Acta Physiol. Scand.* **45**:190.

BENTLEY, P. J. 1961. Directional differences in the permeability to water of the isolated urinary bladder of the toad, *Bufo marinus*. *J. Endocrinol.* **22**:95.

CURRAN, P. F., and J. R. MACINTOSH. 1962. A model system for biological water transport. *Nature.* **193**:347.

DAINTY, J., and C. R. HOUSE. 1966. An examination of the evidence for membrane pores in frog skin. *J. Physiol., (London).* **185**:172.

DAVIS, L. E., and B. SCHMIDT-NIELSEN. 1967. Ultrastructure of the crocodile kidney (*Crocodylus acutus*) with special reference to electrolyte and fluid transport. *J. Morphol.* **121**:255.

DERJAGUIN, B. V. 1965. Recent research into the properties of water in thin films and in microcapillaries. *Symp. Soc. Exptl. Biol.* **19**:55.

DIAMOND, J. M. 1962. The mechanism of water transport by the gall-bladder. *J. Physiol., (London).* **161**:503.

DIAMOND, J. M. 1964. The mechanism of isotonic water transport. *J. Gen. Physiol.* **48**:15.

DURBIN, R. P., H. FRANK, and A. K. SOLOMON. 1956. Water flow through frog gastric mucosa. *J. Gen. Physiol.* **39**:535.

HENNIKER, G. 1949. Depth of the surface zone of a liquid. *Rev. Mod. Phys.* **21**:322.

KAYE, G. I., H. O. WHEELER, R. T. WHITLOCK, and N. LANE. 1966. Fluid transport in the rabbit gall bladder. *J. Cell Biol.* **30**:237.

KOMNICK, H. 1965. Funktionelle Morphologie von Salzdrüsenzellen. *In* Sekretion und Exkretion. Springer Verlag, Berlin.

KUNZ, K. S. 1957. Numerical Analysis. McGraw-Hill Book Company, New York.

PATLAK, C. S., D. A. GOLDSTEIN, and J. F. HOFFMAN. 1963. The flow of solute and solvent across a two-membrane system. *J. Theoret. Biol.* **5**:426.

RALSTON, A., and H. S. WILF. 1960. Mathematical Methods for Digital Computers. John Wiley & Sons Inc., New York.

ROBERTS, J. S., and B. SCHMIDT-NIELSEN. 1966. Renal ultrastructure and excretion of salt and water by three terrestrial lizards. *Am. J. Physiol.* **211**:476.

SCHMIDT-NIELSEN, K. 1960. The salt-secreting gland of marine birds. *Circulation.* **21**:955.

SMYTH, D. H., and E. M. WRIGHT. 1966. Streaming potentials in the rat small intestine. *J. Physiol., (London).* **182**:591.

TORMEY, J. MC.D. 1966. Significance of the histochemical demonstration of ATPase in epithelia noted for active transport. *Nature.* **210**:820.

TORMEY, J. MC.D., and J. M. DIAMOND. 1967. The ultrastructural route of fluid transport in rabbit gall bladder. *J. Gen. Physiol.* **50**:2031.

WHITLOCK, R. T., and H. O. WHEELER. 1964. Coupled transport of solute and water across rabbit gall bladder epithelium. *J. Clin. Invest.* **43**:2249.

WHITTEMBURY, G., D. E. OKEN, E. E. WINDHAGER, and A. K. SOLOMON. 1959. Single proximal tubules of Necturus kidney. IV. Dependence of H_2O movement on osmotic gradients. *Am. J. Physiol.* **197**:1121.